A Carrier Tracking Loop Using Adaptive Strong Tracking Kalman Filter in GNSS Receivers

Yan Cheng and Qing Chang

***Abstract*— The Kalman filter (KF) has been widely used in the carrier track to improve the tracking performance of receivers under challenging environments. The KF-based tracking assumes that the noise statistics are exactly known in advance and kept fixed during the whole iteration process. However, the noise statistics are difficult to know accurately and the fixed noise statistics cannot reflect the practical situations under time-varying environments. To further enhance the performance of carrier tracking, the adaptive strong tracking Kalman filter (STKF) is proposed. The adaptive fading factors are employed in the state prediction covariance to adjust the Kalman gain. Moreover, to improve the accuracy of fading factors in STKF tracking, the measurement noise covariance is adjusted based on the C/N_0 estimations. In addition, the working state is checked, and fading factors are used only when the system is not steady. The proposed algorithm has been implemented in the software receiver. The test results demonstrate that the proposed method has more superior tracking performance under challenging environments than other tracking methods.**

***Index Terms*— GNSS receivers, carrier tracking, KF-based tracking, strong tracking Kalman filter (STKF).**

I. Introduction

FOR the global navigation satellite system (GNSS) receivers, the carrier tracking loop is used to synchronize the local carrier with the incoming signals, which is a significantly important part. The phase lock loop (PLL) is commonly used in the carrier tracking loop, but it is extremely fragile especially under challenging environments. To enhance tracking performance under harsh environments, the Kalman filter (KF) has been applied in the tracking loop to achieve robust tracking [1]. Several studies have shown that the KF-based tracking outperforms the PLL tracking under harsh conditions [1], [2].

However, the performance of KF heavily relies on the precise knowledge of the system and measurement models and noise statistics. Unfortunately, due to the complicated environment in the tracking system, accurate models and noise statistics are difficult to be known. In the KF-based tracking, the noise covariances are initialized before the iteration and remain fixed during the filtering process. However, when the external environment is changing, the fixed noise covariances cannot reflect the real situations. The KF tracking is difficult to track these changes fast or obtain optimal estimations in the variable conditions.

To solve these problems, different adaptive Kalman filter (AKF) methods have been employed to improve KF tracking performance under unknow noise statistics and models. In [3], the tuning scheme was employed in KF tracking. However, this method requires knowledge and experience to select the scale factor to set equivalent noise bandwidth, so its tuning process is not easy. In [4] and [5], the AKF was performed in the carrier tracking to improve the tracking robustness under the ionospheric scintillation conditions, however, these AKF algorithms are just suitable for ionospheric scintillations. In [6], the AKF algorithm for the carrier tracking loop is just designed for the static weak signal conditions. Accordingly, there are few appropriate and easy AKF tracking algorithms for dynamic and weak signal situations in the literature. Dynamic and weak signal conditions often occur in the city canyon, in which the signal power and Doppler frequency are varying simultaneously and often suffering mutations. KF-based tracking method has difficulty to track this variable signal well.

Among many AKF algorithms, strong tracking Kalman filter (STKF) can improve KF robustness against system parameter mismatches, and model errors caused by the mutations [7]. STKF is easy to design and can achieve better performance in navigation integration processing [8]. Although STKF has been widely used in the integrated inertial navigation system, its application in the carrier tracking of GNSS receivers for challenging environments has not been found in the literature. However, STKF is not always effective to deal with inaccurate models because the decision rule in STKF may be activated false (false alarm) or missing activated [9]. Hence, it is necessary to improve STKF in the carrier tracking system to be more intelligent to deal with mismatched models.

In this letter, we propose an adaptive STKF (ASTKF)-based carrier tracking algorithm to improve the tracking performance under dynamic and weak signal conditions. The novel contributions are:

1) To improve the STKF tracking, the measurement noise covariance $\mathbf{R}$ is adjusted by the C/N_0 estimations, which can improve the accuracy of the fading factors.

2) The chi-square test is employed to check the working state and determine whether the fading factor should be used. This can avoid false alarms of STKF and improve filter accuracy.

3) The proposed ASTKF tracking can achieve more superior tracking performance under weak and dynamic signal conditions than the KF tracking and STKF tracking without working state detection and $\mathbf{R}$ adaptation.

II. KF-Based Carrier Tracking Loop

A. State Model and Measurement Model

In the third-order KF-based carrier tracking loop, the state vector $\mathbf{x}_k$ and system transition matrix $\mathbf{\Phi}$ are defined as:

$$\mathbf{x}_k = [\,\Delta\varphi_k \quad \omega_k \quad \alpha_k\,]^{\mathrm{T}} \tag{1}$$

$$\mathbf{\Phi} = \begin{bmatrix} 1 & T & T^2/2 \\ 0 & 1 & T \\ 0 & 0 & 1 \end{bmatrix} \tag{2}$$

Manuscript received July 5, 2020; accepted August 13, 2020. Date of publication August 24, 2020; date of current version December 10, 2020. This work was funded by the National Natural Science Foundation of China (61471021). The associate editor coordinating the review of this letter and approving it for publication was M. Oner. *(Corresponding author: Qing Chang.)*

The authors are with the School of Electronic and Information Engineering, Beihang University, Beijing 100191, China (e-mail: chengyan178@163.com; changq@263.net).

Digital Object Identifier 10.1109/LCOMM.2020.3018742

where $\Delta\varphi_k$, ω_k and α_k represent carrier phase error in radians, carrier Doppler error in rad/s and carrier Doppler rate in rad/s^2, respectively. T is the update period. Hence, the state model is:

$$\begin{bmatrix} \Delta\varphi_k \\ \omega_k \\ \alpha_k \end{bmatrix} = \begin{bmatrix} 1 & T & T^2/2 \\ 0 & 1 & T \\ 0 & 0 & 1 \end{bmatrix} \begin{bmatrix} \Delta\varphi_{k-1} \\ \omega_{k-1} \\ \alpha_{k-1} \end{bmatrix} + \mathbf{n}_{k-1} \tag{3}$$

where $\mathbf{n}_{k-1}$ represents process noise matrix, and the covariance matrix $\mathbf{Q}_k$ of $\mathbf{n}_k$ is [10]

$$\mathbf{Q}_k = \omega_{rf}^2 \begin{bmatrix} Tq_b + \frac{T^3}{3}q_d + \frac{T^5}{20}\frac{q_a}{C^2} & \frac{T^2}{2}q_d + \frac{T^4}{8}\frac{q_a}{C^2} & \frac{T^3}{6}\frac{q_a}{C^2} \\ \frac{T^2}{2}q_d + \frac{T^4}{8}\frac{q_a}{C^2} & Tq_d + \frac{T^3}{3}\frac{q_a}{C^2} & \frac{T^2}{2}\frac{q_a}{C^2} \\ \frac{T^3}{6}\frac{q_a}{C^2} & \frac{T^2}{2}\frac{q_a}{C^2} & T\frac{q_a}{C^2} \end{bmatrix} \tag{4}$$

where ω_{rf} represents the nominal carrier frequency in rad/s. C represents the speed of light. q_a is the power spectral density of the random walk process noise in (m^2/s^6)/Hz, which is decided by the line-of-light acceleration. q_d and q_b represent the power spectral density of the carrier frequency noise and carrier phase noise, respectively, which are caused by the local oscillator noise and can be obtained by h-parameters of the oscillator [11].

In the KF tracking loop, the measurement $\mathbf{z}_k$ is the output of the phase discriminator. The measurement matrix $\mathbf{H}$ is

$$\mathbf{H} = \begin{bmatrix} 1 & T/2 & T^2/6 \end{bmatrix} \tag{5}$$

Therefore, the measurement equation is described as follows:

$$\delta\varphi_k = \begin{bmatrix} 1 & T/2 & T^2/6 \end{bmatrix} \begin{bmatrix} \Delta\varphi_k \\ \omega_k \\ \alpha_k \end{bmatrix} + v_k \tag{6}$$

where $\delta\varphi_k$ is the measurement vector obtained by a two-quadrant arctangent discriminator. v_k represents zero-mean Gaussian white measurement noise with the covariance $\mathbf{R}_k$.

B. KF Iteration Process

The KF recursive process contains the prediction process and the correction process. The prediction process is as follows [11]:

$$\hat{\mathbf{x}}_k^- = \mathbf{\Phi}\hat{\mathbf{x}}_{k-1} \tag{7}$$

$$\hat{\mathbf{P}}_k^- = \mathbf{\Phi}\hat{\mathbf{P}}_{k-1}\mathbf{\Phi}^{\mathrm{T}} + \mathbf{Q}_{k-1} \tag{8}$$

where $\hat{\mathbf{x}}_k^-$ and $\hat{\mathbf{P}}_k^-$ are predicted estimation and covariance matrix of the state vector, and $\hat{\mathbf{x}}_{k-1}$ and $\hat{\mathbf{P}}_{k-1}$ are estimated state values and covariance matrix. The correction process is [11]:

$$\mathbf{K}_k = \hat{\mathbf{P}}_k^-\mathbf{H}^{\mathrm{T}}\left(\mathbf{H}\hat{\mathbf{P}}_k^-\mathbf{H}^{\mathrm{T}} + \mathbf{R}_k\right)^{-1} \tag{9}$$

$$\hat{\mathbf{x}}_k = \hat{\mathbf{x}}_k^- + \mathbf{K}_k\left(\mathbf{z}_k - \mathbf{H}\hat{\mathbf{x}}_k^-\right) \tag{10}$$

$$\hat{\mathbf{P}}_k = \left(\mathbf{I} - \mathbf{K}_k\mathbf{H}\right)\hat{\mathbf{P}}_k^- \tag{11}$$

where $\mathbf{K}_k$ is the Kalman gain.

III. Proposed Adaptive STKF-Based Carrier Tracking

For the KF, the noise statistics and the Kalman gain remain unchanged when the system converges to the steady state. When the incoming signal is changed, KF is difficult to track the changes quickly. For the carrier tracking system, the noise statistics are varying and are difficult to obtain when receivers operate in harsh environments with mutations. Hence, the models of the KF tracking cannot fit with the harsh conditions, then the mismatched model may result in incorrect Doppler estimations and even losing lock in the tracking process. Therefore, an ASTKF-based tracking algorithm is proposed to improve the tracking performance in challenging environments.

A. Strong Tracking Kalman Filter

The innovation sequence is defined as:

$$\mathbf{d}_k = \mathbf{z}_k - \mathbf{H}\hat{\mathbf{x}}_k^- \tag{12}$$

STKF should satisfy the orthogonal principle [7]:

$$\mathrm{E}[(\mathbf{x}_k - \hat{\mathbf{x}}_k)(\mathbf{x}_k - \hat{\mathbf{x}}_k)^{\mathrm{T}}] = \min \tag{13}$$

$$\mathrm{E}[\mathbf{d}_{k+j}\mathbf{d}_k^T] = 0, \quad j = 1, 2\cdots \tag{14}$$

The estimation of KF depends heavily on past data, which may cause the filter divergence when the external environment changes. STKF introduces fading factors into the state prediction covariance, that is

$$\hat{\mathbf{P}}_k^- = \boldsymbol{\lambda}_k\mathbf{\Phi}\hat{\mathbf{P}}_{k-1}\mathbf{\Phi}^{\mathrm{T}} + \mathbf{Q}_{k-1} \tag{15}$$

where $\boldsymbol{\lambda}_k = \mathrm{diag}(\lambda_{1,k}, \lambda_{2,k}\cdots, \lambda_{n,k})$ are the fading factors. Then, $\hat{\mathbf{P}}_k^-$ is applied in equation (9) to obtain the Kalman gain $\mathbf{K}_k$. Therefore, STKF can adjust the Kalman gain in real-time based on the input measurements. The fading factors $\boldsymbol{\lambda}_k = \mathrm{diag}(\lambda_{1,k}, \lambda_{2,k}\cdots, \lambda_{n,k})$ are given by

$$\lambda_{i,k} = \begin{cases} \sigma_i c_k, & \sigma_i c_k > 1 \\ 1, & \sigma_i c_k \le 1 \end{cases}, \quad i = 1, 2\cdots, n \tag{16}$$

$$c_k = \mathrm{tr}[\mathbf{N}_k] \Big/ \left(\sum_{i=1}^{n} \sigma_i \mathbf{M}_{k,ii}\right) \tag{17}$$

Matrices $\mathbf{N}_k$ and $\mathbf{M}_k$ are defined as follows:

$$\mathbf{N}_k \triangleq \mathbf{V}_k - \mathbf{R}_k - \mathbf{H}\mathbf{Q}_{k-1}\mathbf{H}^{\mathrm{T}} \tag{18}$$

$$\mathbf{M}_k \triangleq \mathbf{H}\mathbf{\Phi}\hat{\mathbf{P}}_{k-1}\mathbf{\Phi}^{\mathrm{T}}\mathbf{H}^{\mathrm{T}} \tag{19}$$

$$\mathbf{V}_k = \begin{cases} \mathbf{d}_1\mathbf{d}_1^{\mathrm{T}}, & k = 1 \\ \left(\rho\mathbf{V}_{k-1} + \mathbf{d}_k\mathbf{d}_k^T\right)/(1+\rho), & k > 1 \end{cases} \tag{20}$$

where $\mathbf{V}_k$ represents the estimated innovation covariance. tr[•] denotes the trace of a matrix. ρ is the forgetting factor and is typically 0.95. σ_i is the predetermined constant, with $\sigma_i \geq 1$, $i = 1,2,\ldots,n$.

For the STKF, the $\mathbf{R}_k$ is assumed to be fixed during the iteration process [7]. However, the decision rule $\sigma_i c_k > 1$ and the accuracy of fading factors may be affected by the inaccurate $\mathbf{R}_k$ in the variable environments. Hence, to improve the STKF-based carrier tracking performance, the adaptive $\mathbf{R}_k$ is introduced in the STKF-based carrier tracking system.

B. Adaptive R_k for STKF-Based Carrier Tracking

According to equations from (16) to (19), because $\hat{\mathbf{P}}_{k-1}$, $\mathbf{\Phi}$ and $\mathbf{H}$ are the positive definite matrices, the $\mathbf{H\Phi}\hat{\mathbf{P}}_{k-1}\mathbf{\Phi}^{\mathrm{T}}\mathbf{H}^{\mathrm{T}}$ is also a positive definite matrix and $\mathrm{tr}(\mathbf{H\Phi}\hat{\mathbf{P}}_{k-1}\mathbf{\Phi}^{\mathrm{T}}\mathbf{H}^{\mathrm{T}}) > 0$. Therefore, the fading factors may be used only when [7]

$$\mathrm{tr}(\mathbf{N}_k) > 0 \tag{21}$$

that is

$$\mathrm{tr}(\mathbf{V}_k - \mathbf{R}_k - \mathbf{HQ}_{k-1}\mathbf{H}^{\mathrm{T}}) > 0 \tag{22}$$

Then, it can be obtained:

$$\mathrm{tr}(\mathbf{V}_k - \mathbf{HQ}_{k-1}\mathbf{H}^{\mathrm{T}}) > \mathrm{tr}(\mathbf{R}_k) \tag{23}$$

Accordingly, the fading factors may put into operation only when inequality (23) can hold. Hence, $\mathbf{R}_k$ is very important to determine the fading factors. If $\mathbf{R}_k$ is not appropriate, the inequality (23) cannot hold and the decision rule $\sigma_i c_k > 1$ may be activated unsuccessfully (alarm failure). In addition, if the (23) can hold and the decision rule can be activated, the wrong $\mathbf{R}_k$ can cause wrong fading factors and reduce the filter accuracy compared with KF. Therefore, inaccurate $\mathbf{R}_k$ may lead to alarm failure or wrong filtering estimations, which is worse than KF.

Therefore, it is necessary to update the $\mathbf{R}_k$ adaptively according to the time-varying environments in the STKF-based tracking. For the carrier tracking loop, the carrier phase discriminator is the two-quadrant arctangent discriminator:

$$\Delta\theta_k = \arctan\left(Q_k / I_k\right) \tag{24}$$

where $\Delta\theta_k$ is the carrier phase error, I_k and Q_k are the correlated signals between the local signal and the received signal of in-phase and quadrature branch at the *kth* epoch.

The main sources of measurement error in the carrier tracking loop are phase jitter and dynamic stress error. The noise variance of the arctangent discriminator output is [10]:

$$\mathbf{R}_k = \mathrm{E}\left[v_k^2\right] = \frac{1}{2T(c/n_0)_k}\left(1 + \frac{1}{2T(c/n_0)_k}\right) \tag{25}$$

where $(c/n_0)_k$ is the carrier-to-noise power ratio at the kth epoch. Moreover, $(c/n_0)_k = 10^{(C/N_0)_k/10}$, where $(C/N_0)_k$ is in dB-Hz. For GNSS receivers, the $(C/N_0)_k$ can be estimated according to the input signals. The estimation method is based on the narrowband-wideband power ratio method (NWPR) [13], which is widely used in the GNSS receivers.

C. Detection of the Working State

The STKF implements the fading factor once $\sigma_i c_k > 1$ in (16) without considering the filter is working optimally or not. If the filter is working in steady state, the decision rule $\sigma_i c_k > 1$ may also be activated false [9]. False alarm can reduce the accuracy of the filter and even lead to filtering divergence. Therefore, it is necessary to detect whether the filter is working steadily or not. Two hypotheses are introduced: H_0: The system is working in the steady state; H_1: There is uncertainty in the system.

The statistic γ_k is defined as:

$$\gamma_k = \mathbf{d}_k^{\mathrm{T}}\hat{\mathbf{C}}_k^{-1}\mathbf{d}_k \tag{26}$$

where $\hat{\mathbf{C}}_k$ is the estimated innovation covariance. If the filter works well, the innovation $\mathbf{d}_k$ will be a Gaussian white noise sequence [12]. Hence, the γ_k obeys the $\chi^2(s)$ distribution with s degrees of freedom, where s is the dimension of $\mathbf{d}_k$.

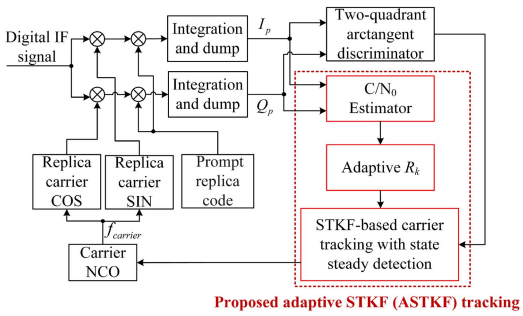

Fig. 1. Block diagram of proposed ASTKF-based tracking loop.

When the significance level α is selected, then

$$\mathrm{P}\left\{\chi^2 \geq \chi_\alpha^2(s)\right\} = \alpha, \quad 0 < \alpha < 1 \tag{27}$$

where the threshold value $\chi_\alpha^2(s)$ can be determined by the chi-square distribution table according to α and *s*. If the hypothesis H_1 is established, $\gamma_k \geq \chi_\alpha^2(s)$. That means the innovation is abnormal and the filter is not working in steady state. Otherwise, the innovation is normal and the filter works well.

For the STKF-based carrier tracking system, the measurement vector $\mathbf{z}_k$ is carrier phase error $\Delta\theta_k$ in (24) which is a scalar in the *kth* epoch. According to (12) and (26), the statistic γ_k and $\mathbf{d}_k$ are both scalars at the *kth* epoch. Then

$$\gamma_k = d_k^{\mathrm{T}}\hat{C}_k^{-1}d_k = d_k^2/\hat{C}_k \sim \chi^2(1) \tag{28}$$

D. The Proposed ASTKF-Based Carrier Tracking Loop

Fig. 1 shows the block diagram of the proposed ASTKF tracking loop. The digital intermediate frequency (IF) signal is divided into two branches, which are multiplied by the in-phase and quadrature local replica carrier signal and the prompt replica code to generate I and Q correlated signals. After the integration and dump block, the integration values of prompt branch I_p and Q_p are sent to the phase discriminator and the C/N_0 estimator. The output of the discriminator is sent to the carrier tracking model. The C/N_0 estimations can adjust the measurement noise covariance $\mathbf{R}_k$ in real-time, which is used to tune the STKF tracking model. Then, the output of the ASTKF-based tracking is employed to update the frequency and phase of the carrier NCO (numerically controlled oscillator).

Fig. 2 presents the proposed ASTKF tracking algorithm. In Fig. 2, the innovation covariance is approximated through averaging inside a moving window of size μ [12],

$$\hat{\mathbf{C}}_k = \frac{1}{\mu}\sum_{\mathrm{i}=k-\mu+1}^{k}\mathbf{d}_i\mathbf{d}_i^T \tag{29}$$

where μ is the length of the window, and $\hat{\mathbf{C}}_k$ is the innovation covariance estimation. To reduce the computational burden, the innovation covariance estimation is obtained by the recursive algorithm [14], that is:

$$\hat{\mathbf{C}}_k = \hat{\mathbf{C}}_{k-1} + \frac{1}{\mu}\left(\mathbf{d}_k\mathbf{d}_k^T - \mathbf{d}_{k-\mu}\mathbf{d}_{k-\mu}^T\right) \tag{30}$$

The multiplication number decreases from μm^2 to $2m^2$, where m is the dimension of the measurement vector. In addition, this innovation covariance estimation not only is used to obtain

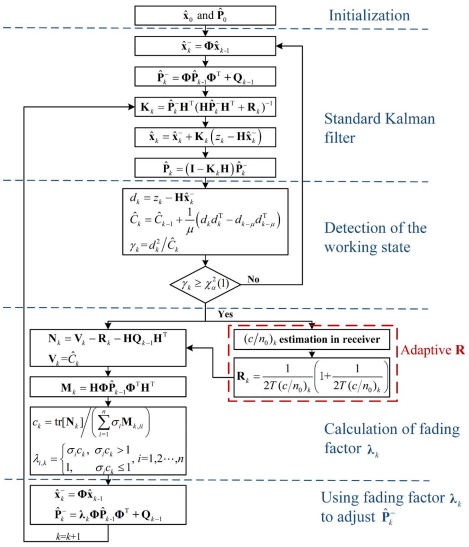

Fig. 2. Flow chart of the proposed ASTKF for carrier tracking loop.

TABLE I
COMPUTATIONAL LOAD FOR VARIABLES IN ASTKF PER ITERATION

Eq.	Variable	Multiplication number	Addition number
(18)	$\mathbf{N}_k$	n^2m+nm^2	$n^2m+nm^2+m^2-nm$
(19)	$\mathbf{M}_k$	$2n^2m+nm+nm^2$	$2n^2m+nm^2-2nm-m^2$
(17)	c_k	$n+1$	$n+m-2$
(12)	$\mathbf{d}_k$	nm	nm
(30)	$\hat{\mathbf{C}}_k$	$3m^2$	$2m^2$
(26)	γ_k	m^2+m	m^2-1

γ_k, but also is used in the STKF to obtain $\mathbf{V}_k$ instead of the equation (20). Therefore, real-time performance can be improved in the ASTKF tracking system.

Compared with KF, the additional computational cost of the ASTKF is composed of two parts: calculation of fading factor and detection of the working state. The most time-consuming part is the calculation of $\mathbf{N}_k$ and $\mathbf{M}_k$. In the calculation of $\mathbf{M}_k$, $\mathbf{\Phi}$ is an upper triangular matrix, which can be used to reduce computational load. The computational requirements of variables in these two parts are shown in Table I. n and m denote the state vector's dimension and measurement vector's dimension. Because $n = 3$ and $m = 1$ in the carrier tracking system model, the number of multiplications $M(n, m)$ and additions $A(n, m)$ for these variables in Table I are:

$$M(n,m) = 3n^2m+2nm^2+2nm+n+4m^2+m+1=48 \tag{31}$$

$$A(n,m) = 3n^2m+2nm^2-2nm+n+m+3m^2-3=31 \tag{32}$$

According to [15], the numbers of multiplication and addition of KF are $2n^3 + 3n^2m + n^2 + 2nm^2 + 2nm = 102$ and $2n^3 + 3n^2m + 2nm^2 - nm - n = 81$. Compared with one iteration required for KF, the increased multiplication number is 47% and the increased addition number is 38% in the ASTKF. Hence, compared with KF, the additional computational load of ASTKF is not heavy.

TABLE II
DESCRIPTION OF THE VEHICLE MOTION FOR CASE 1

Time interval (s)	Motion
[0~99]	Stationary
[100~120]	Constant acceleration of 40 m/s^2
[121~199]	Constant velocity of 800 m/s
[200~220]	Constant deceleration of -32.5 m/s^2
[221~299]	Constant velocity of 150 m/s
[300~325]	1st circular turn
[326~359]	Constant velocity of 150 m/s
[360~376]	2nd circular turn
[377~400]	Constant velocity of 150 m/s
[401~420]	Constant acceleration of 20 m/s^2
[421~450]	Constant velocity of 550 m/s
[451~478]	Constant deceleration of -20 m/s^2

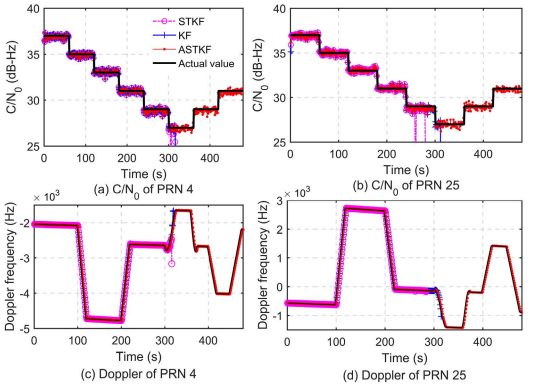

Fig. 3. C/N_0 and Doppler estimations of PRN 4 and PRN 25 in Case 1 (PRN: pseudo-random number).

IV. SIMULATION VERIFICATION

To evaluate the proposed ASTKF carrier tracking algorithm, the tracking method is implemented on a GPS software receiver based on the Visual C++ platform. The simulated IF signal is input to the software receiver. The frequency of the IF signal is 1.42 MHz, the sampling rate is 10 MHz, and the signal resolution is 4-bit.

A. Case 1: Signal Attenuated With Dynamics

Nine visible satellites are simulated in the software receiver. In each channel, signal strength attenuation and dynamics are implemented simultaneously, which is a challenging environment for the carrier tracking loop. For the signal strength, in the first 60 s, the C/N_0 of the signal was set to 37 dB-Hz. Then the signal strength was decreased by 2 dB every 60 s until it reached 27 dB-Hz and was maintained this level for 60 s. Finally, the strength was recovered by 2 dB every 60 s until it reached 31 dB-Hz. For the dynamic, the vehicle motion has been described in Table II. The actual C/N_0 and the dynamics of the signal can be shown in Fig. 3.

The proposed ASTKF-based tracking method is compared with KF-based tracking and STKF-based tracking without the detection of the working state and the adaptive $\mathbf{R}$ model in Fig. 2. For the three algorithms, the initial value of $\mathbf{Q}$ is depended on (4) where $q_a = 0.25$ (m^2/s^6)/Hz and $\mathbf{R}$ is initialized relied on (25) with $C/N_0 = 37$ dB-Hz. The update intervals are set to 4 ms. For the proposed ASTKF-based tracking, the window size μ is set to 20 and the threshold value $\chi^2_{0.02}(1)$ is 5.4119.

Fig. 3 shows the C/N_0 and Doppler frequency estimations for PRN 4 and PRN 25. In Figs. 3(a) and 3(b), the

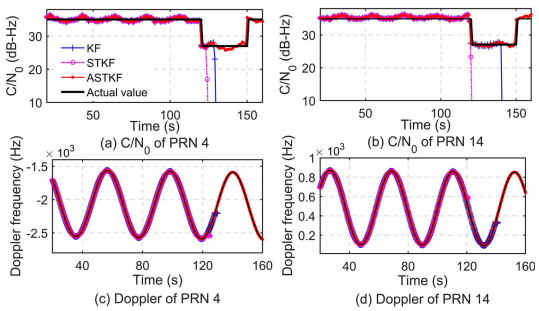

Fig. 4. C/N_0 and Doppler estimations for PRN 4 and PRN 14 in Case 2.

three methods can follow the actual C/N_0 above 29 dB-Hz. In Figs. 3(c) and 3(d), when the signal strength is relatively high and the dynamics only contains acceleration during 100-299 s, the KF and the ASTKF algorithms both can track well. However, the STKF method for PRN 25 loses lock at 284 s. This indicates that without the detection of working state and **R** adaptation, the STKF tracking may lead to false alarm causing inaccurate estimations and then is worse than KF. STKF method cannot introduce appropriate fading factors in all cases. Therefore, it is necessary to improve STKF tracking by introducing the working state detection and **R** adaptation in the carrier tracking system.

When the signal strength is relatively low and the vehicle turns suddenly, the KF method cannot track well and lose lock in this interval. In the first turn during 300-325 s, the KF tracking for PRN 4 and 25 both lose lock, while the proposed ASTKF method can still track well. The proposed method shows a more superior tracking performance under the dynamic weak signal conditions.

B. Case 2: Circular Motion With Interference

In Case 2, the signal C/N_0 started at 35 dB-Hz in the first 120 s. From 121 s to 150 s, the C/N_0 was reduced to 27 dB-Hz. During 151 s to 170 s, the signal was recovered to 35 dB-Hz. This variation of the signal power is to simulate a strong interference environment. For the signal dynamics, the vehicle was simulated to conduct a circular trajectory with a radius of 800 m and a constant velocity of 120 m/s. The actual C/N_0 variation and Doppler frequency of the signal are depicted in Fig. 4. The maximum acceleration and jerk of the signal reach 16.9 m/s^2 and 2.5 m/s^3, respectively. In this simulation, **R** is initialized relied on (25) with C/N_0 =35 dB-Hz. Other parameters are the same as the values in Case 1.

Fig. 4 demonstrates the tracking results for PRN 4 and PRN 14. When the signal strength is relatively high, the receivers with the three tracking algorithms can track the dynamic signal well. However, when the C/N_0 of the signal drops to 27 dB-Hz, the KF tracking and the STKF tracking both lose lock at 27 dB-Hz, while the proposed ASTKF tracking can still track the weak dynamic signal well. For the STKF tracking with fixed **R**, the decision rule $\sigma_i c_k > 1$ is activated by the sudden interference. However, the inaccurate **R** causes inaccurate fading factors, which lead to lose lock and be worse than KF. Therefore, for the carrier tracking system, the proposed ASTKF method shows better tracking performance when the circular motion experiences a sudden interference.

V. Conclusion

This letter proposes a carrier tracking loop based on the ASTKF algorithm to improve the tracking performance under harsh conditions. The proposed ASTKF introduces the working state detection and adjusts **R** by the C/N_0 estimations in the STKF, which is easy to apply without the heavy computational burden. The test results in the software receiver show that the proposed ASTKF tracking method outperforms the KF tracking and STKF tracking under challenging environments.

References

[1] J. A. Lopez-Salcedo, J. A. Del Peral-Rosado, and G. Seco-Granados, "Survey on robust carrier tracking techniques," *IEEE Commun. Surveys Tuts.*, vol. 16, no. 2, pp. 670–688, 2nd Quart., 2014.

[2] D. R. Salem, C. O'Driscoll, and G. Lachapelle, "Methodology for comparing two carrier phase tracking techniques," *GPS Solutions*, vol. 16, no. 2, pp. 197–207, Apr. 2012.

[3] J.-H. Won, "A novel adaptive digital phase-lock-loop for modern digital GNSS receivers," *IEEE Commun. Lett.*, vol. 18, no. 1, pp. 46–49, Jan. 2014.

[4] P. B. S. Harsha and D. V. Ratnam, "Implementation of advanced carrier tracking algorithm using adaptive-extended Kalman filter for GNSS receivers," *IEEE Geosci. Remote Sens. Lett.*, vol. 13, no. 9, pp. 1280–1284, Sep. 2016.

[5] J. Vila-Valls, P. Closas, C. Fernandez-Prades, J. A. Lopez-Salcedo, and G. Seco-Granados, "Adaptive GNSS carrier tracking under ionospheric scintillation: Estimation vs. Mitigation," *IEEE Commun. Lett.*, vol. 19, no. 6, pp. 961–964, Jun. 2015.

[6] Y. Cheng and Q. Chang, "A coarse-to-fine adaptive Kalman filter for weak GNSS signals carrier tracking," *IEEE Commun. Lett.*, vol. 23, no. 12, pp. 2348–2352, Dec. 2019.

[7] D. H. Zhou and P. M. Frank, "Strong tracking filtering of nonlinear time-varying stochastic systems with coloured noise: Application to parameter estimation and empirical robustness analysis," *Int. J. Control*, vol. 65, no. 2, pp. 295–307, Sep. 1996.

[8] D.-J. Jwo and S.-H. Wang, "Adaptive fuzzy strong tracking extended Kalman filtering for GPS navigation," *IEEE Sensors J.*, vol. 7, no. 5, pp. 778–789, May 2007.

[9] Q. Ge, T. Shao, C. Wen, and R. Sun, "Analysis on strong tracking filtering for linear dynamic systems," *Math. Problems Eng.*, vol. 2015, pp. 1–9, Sep. 2015.

[10] C. O'Driscoll, M. G. Petovello, and G. Lachapelle, "Choosing the coherent integration time for Kalman filter-based carrier-phase tracking of GNSS signals," *GPS Solutions*, vol. 15, no. 4, pp. 345–356, Oct. 2011.

[11] R. G. Brown and P. Y. C. Hwang, *Introduction to Random Signals and Applied Kalman Filtering*, 4th ed. Hoboken, NJ, USA: Wiley, 2012, pp. 324–327.

[12] A. H. Mohamed and K. P. Schwarz, "Adaptive Kalman filtering for INS/GPS," *J. Geodesy*, vol. 73, no. 4, pp. 193–203, May 1999.

[13] E. Falletti, M. Pini, and L. L. Presti, "Low complexity carrier-to-noise ratio estimators for GNSS digital receivers," *IEEE Trans. Aerosp. Electron. Syst.*, vol. 47, no. 1, pp. 420–437, Jan. 2011.

[14] E. Zerdali, "Adaptive extended Kalman filter for speed-sensorless control of induction motors," *IEEE Trans. Energy Convers.*, vol. 34, no. 2, pp. 789–800, Jun. 2019.

[15] K. Lo, Q. Lu, and W. Hyun Kwon, "Comments on 'optimal solution of the two-stage Kalman estimator," *IEEE Trans. Autom. Control*, vol. 47, no. 1, pp. 198–199, Jan. 2002.